

Note on the thermodynamic Bethe ansatz approach to the quantum phase diagram of the strong coupling ladder compounds

This content has been downloaded from IOPscience. Please scroll down to see the full text.

2003 New J. Phys. 5 107

(<http://iopscience.iop.org/1367-2630/5/1/107>)

View [the table of contents for this issue](#), or go to the [journal homepage](#) for more

Download details:

IP Address: 143.54.42.15

This content was downloaded on 23/04/2015 at 17:54

Please note that [terms and conditions apply](#).

Note on the thermodynamic Bethe ansatz approach to the quantum phase diagram of the strong coupling ladder compounds

M T Batchelor^{1,2}, X-W Guan^{1,2}, A Foerster³ and H-Q Zhou⁴

¹ Department of Theoretical Physics, Research School of Physical Sciences and Engineering, Australian National University, Canberra, ACT 0200, Australia

² Centre for Mathematics and its Applications, Mathematical Sciences Institute, Australian National University, Canberra, ACT 0200, Australia

³ Instituto de Física da UFRGS, Avenida Bento Gonçalves 9500, Porto Alegre, RS, Brazil

⁴ Centre for Mathematical Physics, University of Queensland, Queensland 4072, Australia

E-mail: murrayb@maths.anu.edu.au

New Journal of Physics **5** (2003) 107.1–107.9 (<http://www.njp.org/>)

Received 30 May 2003

Published 11 August 2003

Abstract. We investigate the low-temperature phase diagram of the exactly solved $su(4)$ two-leg spin ladder as a function of the rung coupling J_{\perp} and magnetic field H by means of the thermodynamic Bethe ansatz (TBA). In the absence of a magnetic field the model exhibits three quantum phases, while in the presence of a strong magnetic field there is no singlet ground state for ferromagnetic rung coupling. For antiferromagnetic rung coupling, there is a gapped phase in the regime $H < H_{c1}$, a fully polarized gapped phase for $H > H_{c2}$ and a Luttinger liquid magnetic phase in the regime $H_{c1} < H < H_{c2}$. The critical behaviour derived using the TBA is consistent with the existing experimental, numerical and perturbative results for the strong coupling ladder compounds. This includes the spin excitation gap and the critical fields H_{c1} and H_{c2} , which are in excellent agreement with the experimental values for the known strong coupling ladder compounds $(5\text{IAP})_2\text{CuBr}_4 \cdot 2\text{H}_2\text{O}$, $\text{Cu}_2(\text{C}_5\text{H}_{12}\text{N}_2)_2\text{Cl}_4$ and $(\text{C}_5\text{H}_{12}\text{N})_2\text{CuBr}_4$. In addition we predict the spin gap $\Delta \approx J_{\perp} - \frac{1}{2}J_{\parallel}$ for the weak coupling compounds with $J_{\perp} \sim J_{\parallel}$, such as $(\text{VO})_2\text{P}_2\text{O}_7$, and also show that the gap opens for arbitrary J_{\perp}/J_{\parallel} .

Contents

1	The model	3
2	Ferromagnetic rung coupling	4
3	Strong antiferromagnetic regime	5
4	Magnetization plateau	5
	Acknowledgments	8
	References	8

Recently there has been considerable theoretical and experimental interest in spin ladder systems. With the rapid progress presently being made in nano-engineering, many compounds with a ladder structure have been experimentally realized, such as $\text{SrCu}_2(\text{BO}_3)_2$, $\text{Cu}_2(\text{C}_5\text{H}_{12}\text{N}_2)_2\text{Cl}_4$, $(\text{C}_5\text{H}_{12}\text{N})_2\text{CuBr}_4$ and KCuCl_3 [1]. The existence of a spin gap, magnetization plateaux, superconductivity under hole doping, etc, are examples of some interesting physical properties that may be observed in experiments involving ladder compounds (see, e.g., [1]–[7] and references therein). From the theoretical point of view, most of the results for ladder systems were initially obtained from studies of the standard Heisenberg ladder, which in contrast to its one-dimensional counterpart, cannot be solved exactly. Subsequently, other generalized ladder models have been proposed [8] and analysed through various numerical, approximate and exact approaches [9]–[12].

On the other hand, although some exactly solved or integrable ladder models have been introduced (see, e.g., [13]–[15]), none have so far been used to predict physical properties which could be compared directly with experimental data, such as the critical magnetic fields. In this context, the integrable spin ladder model based on the $su(4)$ algebra [13] appears to be a good candidate for this purpose, since its Hamiltonian consists of the standard Heisenberg ladder model with an extra biquadratic spin interaction term along the legs, the physical importance of which has been noted [8]. In the strong coupling limit, the contribution to the low-temperature physics from the biquadratic term is minimal and, as a consequence, the model exhibits similar critical behaviour to the standard Heisenberg ladder. Therefore it is reasonable to expect that the integrable $su(4)$ ladder model can well describe the low-temperature critical behaviour of the strong coupling ladder materials. In addition, by properly minimizing the intrachain coupling in the integrable ladder Hamiltonian, the model may also be used to describe the weak coupling compounds.

Here we show that this is in fact true in the strong coupling regime by investigating the quantum phase diagram of the integrable $su(4)$ ladder, which can be tested by experiments. Our analytic expression for the gap, $\Delta = J_\perp - 4J_\parallel/\gamma$, and the critical fields, $\mu_B g H_{c1} = \Delta$ and $\mu_B g H_{c2} = J_\perp + 4J_\parallel/\gamma$, where γ is a rescaling constant, can be applied in general to strong coupling ladder compounds with Heisenberg interactions, such as $(\text{SIAP})_2\text{CuBr}_4 \cdot 2\text{H}_2\text{O}$, $\text{Cu}_2(\text{C}_5\text{H}_{12}\text{N}_2)_2\text{Cl}_4$, $(\text{C}_5\text{H}_{12}\text{N})_2\text{CuBr}_4$ and KCuCl_3 , by choosing $\gamma \approx 4$. For weak ($J_\perp \sim J_\parallel$) coupling compounds, such as $(\text{VO})_2\text{P}_2\text{O}_7$, the choice of $\gamma \approx 8$ determines a good fit for the gap [1, 16]. In addition, in the presence of a strong magnetic field, we show that the quantum phase diagram and the critical behaviour predicted from the thermodynamic Bethe ansatz (TBA) are in good agreement with the experimental results for the above-mentioned compounds. We also show that the gap opens for an arbitrary value of J_\perp/J_\parallel , in accordance with the experimental results.

1. The model

We consider the phase diagram of the simplest integrable spin ladder [13]

$$H = \frac{J_{\parallel}}{\gamma} H_{\text{leg}} + J_{\perp} \sum_{j=1}^L \vec{S}_j \vec{T}_j + h \sum_{j=1}^L (S_j^z + T_j^z), \quad (1)$$

where

$$H_{\text{leg}} = \sum_{j=1}^L (\vec{S}_j \vec{S}_{j+1} + \vec{T}_j \vec{T}_{j+1} + 4\vec{S}_j \vec{S}_{j+1} \vec{T}_j \vec{T}_{j+1}). \quad (2)$$

Here \vec{S}_j and \vec{T}_j are the standard spin- $\frac{1}{2}$ operators acting on site j of the upper and lower legs, respectively, J_{\parallel} and J_{\perp} are the intrachain (leg) and interchain (rung) couplings and h is the magnetic field. Throughout, L is the number of rungs and periodic boundary conditions are imposed. Essentially, the competition between the rung and leg couplings and the magnetic field h determines the physical properties and the critical behaviour of the system. In order to facilitate the comparison with real compounds, the intrachain part of this model (2) can be minimized through a rescaling constant γ . In comparison with the standard spin- $\frac{1}{2}$ Heisenberg ladder [1, 2, 3, 17], the above Hamiltonian contains a four-spin interaction term, which minimizes the Haldane phase [8] and causes a shift of the critical value of the rung coupling J_{\perp} at which the model becomes massive. It is well established that this Hamiltonian is integrable and its leg part H_{leg} is (up to a constant) simply the permutation operator corresponding to the $su(4)$ algebra [13]. In addition, after the convenient change of basis, $|1\rangle = \frac{1}{\sqrt{2}}(|\uparrow\downarrow\rangle - |\downarrow\uparrow\rangle)$, $|2\rangle = |\uparrow\uparrow\rangle$, $|3\rangle = \frac{1}{\sqrt{2}}(|\uparrow\downarrow\rangle + |\downarrow\uparrow\rangle)$, $|4\rangle = |\downarrow\downarrow\rangle$, where the first state denotes the rung singlet and the three others the components of the triplet, the leg part remains of the same form while the rung term becomes diagonal. This rung term reduces the $su(4)$ symmetry of H_{leg} to $su(3) \oplus u(1)$ symmetry. Switching on the magnetic field breaks this symmetry further due to Zeeman splitting. This Hamiltonian can be diagonalized using the nested algebraic Bethe ansatz (BA) with three levels. It is worth noting that, for the ladder Hamiltonian (1), the singlet rung state is energetically favoured for $J_{\perp} > 0$, whereas the triplet rung state is favoured for $J_{\perp} < 0$. On applying the magnetic field, component $|2\rangle$ of the triplet is energetically favoured. We will use these properties to our advantage by doing calculations with the choice of ordering for which the BA reference state is the closest to the true ground state of the system.

The underlying BA equations for Hamiltonian (1) are well known [18] and consist of a set of three coupled equations depending on the flavours, v , u and w . Adopting the string conjecture [19, 20] and taking the thermodynamic limit, the densities of the three flavours, $\rho_n^{(1)}(v)$, $\rho_n^{(2)}(u)$ and $\rho_n^{(3)}(w)$, can be defined as usual. After some manipulations, the BA equations reduce to

$$\begin{pmatrix} \ln(1 + \eta_n^{(1)}) \\ \ln(1 + \eta_n^{(2)}) \\ \ln(1 + \eta_n^{(3)}) \end{pmatrix} = \frac{G}{T} + K * \begin{pmatrix} \ln(1 + \eta_m^{(1)-1}) \\ \ln(1 + \eta_m^{(2)-1}) \\ \ln(1 + \eta_m^{(3)-1}) \end{pmatrix}, \quad (3)$$

where $\rho_n^{(1)h}(v)$, $\rho_n^{(2)h}(u)$ and $\rho_n^{(3)h}(w)$ denote the hole densities and

$$K = \begin{pmatrix} \sum_m A_{nm} & -\sum_m a_{nm} & 0 \\ -\sum_m a_{nm} & \sum_m A_{nm} & -\sum_m a_{nm} \\ 0 & -\sum_m a_{nm} & \sum_m A_{nm} \end{pmatrix}, \quad (4)$$

where

$$A_{nm}(\lambda) = \delta(\lambda)\delta_{nm} + (1 - \delta_{nm})a_{|n-m|}(\lambda) + a_{n+m}(\lambda) + 2 \sum_{l=1}^{\min(n,m)-1} a_{|n-m|+2l}(\lambda), \quad (5)$$

$$a_{nm}(\lambda) = \sum_{l=1}^{\min(n,m)} a_{n+m+1-2l}(\lambda), \quad (6)$$

with $a_n(\lambda) = 1/2\pi n/n^2/4 + \lambda^2$. The symbol $*$ denotes convolution and $\eta_n^{(l)}(\lambda) = \rho_n^{(l)h}(\lambda)/\rho_n^{(l)}(\lambda) := \exp(\epsilon_n^{(l)}(\lambda)/T)$, $l = 1, 2, 3$. The dressed energy $\epsilon_n^{(l)}$ plays the role of an excitation energy measured from the Fermi level. The driving matrix G depends on the choice of the reference state. Explicitly, for $J_\perp < 0$, $G = \text{column}(-(J_\parallel/\gamma)2\pi a_n + nh, nh, -(J_\perp + h))$ giving the free energy

$$\frac{F(T, h)}{L} = -h - T \int_{-\infty}^{\infty} \sum_{n=1}^{\infty} a_n(\lambda) \ln(1 + e^{-\epsilon_n^{(l)}(\lambda)/T}) d\lambda. \quad (7)$$

On the other hand, for $J_\perp > 0$, $G = \text{column}(-(J_\parallel/\gamma)2\pi a_n + n(J_\perp - h), nh, nh)$, which leads to the form of the free energy (7) without the field term h . The TBA equations (3) provide a clear physical picture of the ground state and the elementary excitations, as well as the thermodynamic quantities such as the free energy, magnetization, susceptibility, etc. Our results extend the earlier calculations on this model [13, 21].

2. Ferromagnetic rung coupling

In the low-temperature regime $T \rightarrow 0$, only the negative part of the dressed energies $\epsilon^{(l)}$, denoted by $\epsilon^{(l)-}$, contribute to the ground-state energy. The TBA equations (3) then become

$$\begin{aligned} \epsilon^{(1)} &= g_1 - a_2 * \epsilon^{(1)-} + a_1 * \epsilon^{(2)-}, \\ \epsilon^{(2)} &= g_2 - a_2 * \epsilon^{(2)-} + a_1 * [\epsilon^{(1)-} + \epsilon^{(3)-}], \\ \epsilon^{(3)} &= g_3 - a_2 * \epsilon^{(3)-} + a_1 * \epsilon^{(2)-}, \end{aligned} \quad (8)$$

where $g_a, a = 1, 2, 3$, are the driving terms with respect to the basis order. In the regime $J_\perp < 0$, the component $|\uparrow\uparrow\rangle$ of the triplet state is chosen as the reference state. The driving terms are given by $g_1 = -(J_\parallel/\gamma)2\pi a_1 + h$, $g_2 = h$ and $g_3 = -h - J_\perp$, respectively. Thus, in the absence of a magnetic field, the triplet is completely degenerate. The Fermi surface of the singlet is lifted as J_\perp becomes more negative. If J_\perp is negative enough, the singlet rung state is not involved in the ground state, namely $\epsilon^{(3)}(0) \geq 0$, whereas the two other triplet Fermi seas still have their Fermi boundaries at infinity. In such a configuration, we may determine the critical point defining the transition from the $su(4)$ phase into the $su(3)$ phase by solving the TBA equations (8), with the result $J_c^- = -(J_\parallel/\gamma)((\pi/\sqrt{3}) - \ln 3)$. At this critical point the free energy is given by $F(0, 0)/L \approx -(2J_\parallel/3\gamma)(\psi(1) - \psi(\frac{1}{3}))$, indicating a standard $su(3)$ phase. Here $\psi(n)$ is the digamma function. It is worth noting that the critical point J_c^- does not stabilize if an external magnetic field is applied. If the magnetic field is large enough, the ferromagnetic state $|\uparrow\uparrow\rangle$ becomes the true physical ground state, i.e. there is a fully polarized gapped phase. It is found that for $h \geq H_c^F = (4J_\parallel/\gamma)$, the state is fully polarized, provided that $J_\perp \leq -(4J_\parallel/\gamma)$. Therefore, in the ferromagnetic regime, the ground state is in the critical $su(3)$ phase. If the magnetic field is greater than H_c^F , the ground state is ferromagnetic with a magnetization plateau $S^z = 1$.

3. Strong antiferromagnetic regime

In the antiferromagnetic regime, $J_{\perp} > 0$, the rung singlet state is the reference state. Thus the driving terms are given by $g_1 = -(J_{\parallel}/\gamma)2\pi a_1 + J_{\perp} - h$ and $g_2 = g_3 = h$, respectively. From the TBA equations (8), if $h = 0$ we immediately conclude that the triplet excitation is massive with the gap given by $\Delta = J_{\perp} - 4J_{\parallel}/\gamma$ for the regime $J_{\perp} \geq J_c^+ = 4J_{\parallel}/\gamma$. Here J_c^+ is the critical point at which the quantum phase transition from the three branches of the Luttinger liquid phase to the dimerized $u(1)$ phase occurs. To obtain good agreement with the experimental gap, we fix the rescaling constant γ with the coupling constants remaining arbitrary. For the strong coupling compounds, e.g. $(5\text{IAP})_2\text{CuBr}_4 \cdot 2\text{H}_2\text{O}$ [5], $\text{Cu}_2(\text{C}_5\text{H}_{12}\text{N}_2)_2\text{Cl}_4$ [3] and $(\text{C}_5\text{H}_{12}\text{N})_2\text{CuBr}_4$ [4], the experimental gap is well established as $\Delta \approx J_{\perp} - J_{\parallel}$ and, as a consequence, we fix $\gamma \approx 4$. On the other hand, for weak coupling compounds, e.g. $(\text{VO})_2\text{P}_2\text{O}_7$ [1, 16], the choice of $\gamma \approx 8$ determines a good fit with the gap $\Delta \approx \frac{1}{2}J_{\perp}$. We stress that the purpose of introducing the rescaling constant is to minimize the effects of the biquadratic term, so that the model lies in the same Haldane phase as the pure Heisenberg ladder.

4. Magnetization plateau

The phase diagram of the antiferromagnetic spin ladders in the presence of a magnetic field is particularly interesting, because the critical points can be measured through critical magnetic fields. The appearance of quantized magnetization plateaus in the presence of a strong magnetic field is expected on general grounds [1]. From the TBA equations (8) for antiferromagnetic rung coupling we observe that the magnetic field lifts the Fermi seas of $\epsilon^{(2)}$ and $\epsilon^{(3)}$. If $J_{\perp} > J_c^+$, we can show that the two components of the triplet states, $|3\rangle$ and $|4\rangle$, do not become involved in the ground state for a strong magnetic field. Basically, the magnetic field lifts the component $|2\rangle$ of the triplet closer to the singlet ground state such that they form a new effective spin- $\frac{1}{2}$ state. Therefore, in a strong magnetic field the ground state may be considered as a condensate of $su(2)$ hard-core bosons. The gap can be deduced via the magnetic field h : the first critical field occurs at H_{c1} , where $g\mu_B H_{c1} = \Delta$, i.e. the magnetic field closes the gap. The quantum phase transition from a gapped to a gapless Luttinger phase occurs. However, by continuing to increase the magnetic field h above the first critical field H_{c1} , the component $|2\rangle$ of the triplet becomes involved in the ground state with a finite susceptibility. If the magnetic field is greater than the rung coupling, i.e. $h > J_{\perp}$, the state $|2\rangle$ becomes the lowest level. Therefore, it is reasonable to choose the basis order as $(|2\rangle, |1\rangle, |3\rangle, |4\rangle)^T$. Subsequently the driving terms are given by $g^{(1)} = -2\pi J_{\parallel}a_1 - J_{\perp} + h$, $g^{(2)} = J_{\perp}$ and $g^{(3)} = h$. From the TBA, we see that the ground state is a fully polarized ferromagnetic state when the magnetic field is greater than $H_{c2} = J_{\perp} + 4J_{\parallel}/\gamma$. Indeed, the critical field H_{c2} is in excellent agreement with the experimental data for the very strong coupling compound $(5\text{IAP})_2\text{CuBr}_4 \cdot 2\text{H}_2\text{O}$ (abbreviated as B5i2aT), [5] and in a good agreement with the strong coupling compounds $\text{Cu}_2(\text{C}_5\text{H}_{12}\text{N}_2)_2\text{Cl}_4$ (abbreviated Cu(Hp)Cl) [3] and $(\text{C}_5\text{H}_{12}\text{N})_2\text{CuBr}_4$ (abbreviated BPCN) [4] (see table 1). On the other hand, the precise structure of the compound KCuCl_3 is not clear [1]. It is believed to exhibit a double-chain structure [6] with a gap $\Delta \approx 35$ K identified via the best fitting in the susceptibility curve through the Troyer formula [22]. The coupling constants are determined as $J_{\perp} = 4J_{\parallel}$, $J_{\parallel} = 12.3$ K, $J_{\text{diag}} = 0$ [6]. However, high-field measurements indicate the gap $\Delta \approx 31.1$ K [7]. Our TBA result gives poor agreement with the experimental result for this type of ladder compound (see table 1). This suggests that the compound may exhibit a double-chain

Table 1. Comparison between the experimental values for the critical points H_{c1} and H_{c2} for strong coupling ladder compounds and the TBA results obtained from the $su(4)$ integrable model.

Compounds	g	J_{\perp} (K)	J_{\parallel} (K)	γ	H_{c1} (exp) (T)	H_{c2} (exp) (T)	H_{c1} (TBA) (T)	H_{c2} (TBA) (T)
B5i2aT	2.1	13	1.15	4	8.4	10.4	8.3	10.03
Cu(Hp)Cl	2.03	13.2	2.5	4	7.5	13.2	7.84	11.51
BPCB	2.13	13.3	3.8	4	6.6	14.6	6.6	11.95
KCuCl ₃	2.05	49.2	12.3	2.68	22.4	≈ 60	22.4	49

structure with additional diagonal interaction. For these double-chain structure ladders, such as KCuCl₃, TiCuCl₃, etc, the leg couplings appear to be very large, resulting in a discrepancy with the critical fields derived from the TBA method.

After a similar calculation, we obtain the magnetization $S^z \approx 4Q_1(1 - 2Q_1/\pi)/\pi$ in the vicinity of the critical field H_{c1} , with the Fermi boundary $Q_1 \approx \sqrt{(h - H_{c1})/(H_{c1} - 5h)}$. For a very strong magnetic field such that $H_{c2} - h \ll 1$ the free energy is

$$\frac{F(0, h)}{L} \approx -h - \frac{4(H_{c2} - h)^{3/2}}{\pi \sqrt{5h - H_{c2}}} \quad (9)$$

and the susceptibility $\kappa \approx (3/\pi \sqrt{4H_{c2}})(H_{c2} - h)^{-1/2}$, which indicates the nature of the singular behaviour in a phase transition from a gapless to a ferromagnetic phase. The magnetization is given by $S^z \approx 1 - 4Q_2(1 - 2Q_2/\pi)/\pi$, where $Q_2 \approx \sqrt{(H_{c2} - h)/(5h - H_{c2})}$. The fact that the magnetization depends on the square root of the field in the vicinity of the critical fields is consistent with other theoretical [11, 12] and numerical results [9]. The magnetization increases almost linearly between the critical fields H_{c1} and H_{c2} . The ground state is ferromagnetic above H_{c2} with the gap $\Delta = \mu g(H - H_{c2})$.

Numerical solution of the TBA equations gives a reasonable magnetization curve (see figure 1) which passes through an inflection point midway between H_{c1} and H_{c2} . This inflection point is clearly visible in experimental curves, e.g. for $(5\text{IAP})_2\text{CuBr}_4 \cdot 2\text{H}_2\text{O}$ [5], $\text{Cu}_2(\text{C}_5\text{H}_{12}\text{N}_2)_2\text{Cl}_4$ [3] and $(\text{C}_5\text{H}_{12}\text{N})_2\text{CuBr}_4$ [4]. The physical meaning of the inflection point is that the probabilities of the singlet and the triplet states $|2\rangle$ in the ground state are equal. It suggests an ordered dimer state close to half-filling [23]. Therefore, in the strong coupling regime, the one-point correlation function $\langle S_j \cdot T_j \rangle = -\frac{3}{4}$ lies in a gapped singlet ground state, which indicates an ordered dimer phase, while $\langle S_j \cdot T_j \rangle = \frac{1}{4}$ is in the fully polarized ferromagnetic phase. However, in a Luttinger liquid phase, we find $\langle S_j \cdot T_j \rangle = -\frac{3}{4} + S^z$. The magnetic field increases the one-point correlation function.

We also notice that our results for the gap, $\Delta = J_{\perp} - 4J_{\parallel}/\gamma$, and the critical field, $H_{c2} = J_{\perp} + 4J_{\parallel}/\gamma$, coincide for $\gamma = 4$ with the first-order perturbation theory results obtained for strong coupling [11]. However, their higher-order terms lead to poor agreement with the experimental results. It is apparent that the rescaling constant γ causes a shift in the critical point. This can be seen from the values of

$$H_{c2}/\Delta = 1 + 2 \left/ \left(\frac{\gamma J_{\perp}}{4J_{\parallel}} - 1 \right) \right., \quad (10)$$

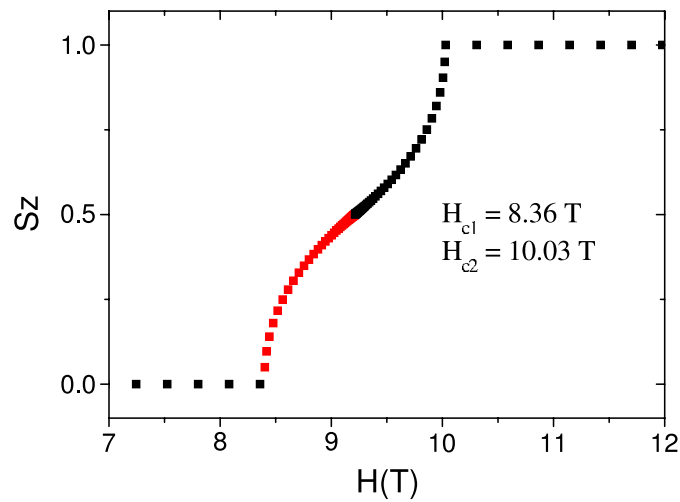


Figure 1. Magnetization S^z versus magnetic field $H = \mu_B g h$ obtained from the TBA equations for the values $J_{\perp} = 13$ K, $J_{\parallel} = 1.15$ K and $\gamma = 4$ for the strong coupling compound $(5\text{IAP})_2\text{CuBr}_4 \cdot 2\text{H}_2\text{O}$ [5]. At the inflection point $h = J_{\perp}$ the magnetization is 0.5. The curve is in excellent agreement with the experimental result [5].

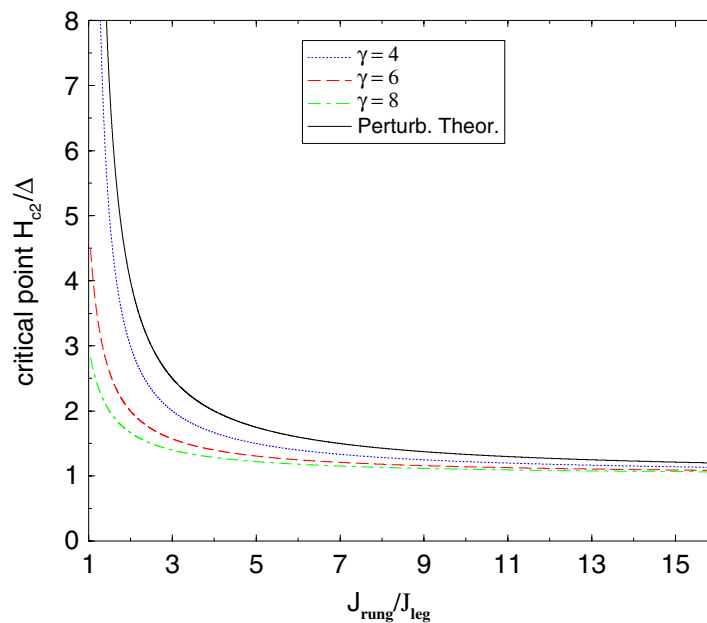


Figure 2. The critical point H_{c2}/Δ as a function of the ratio J_{\perp}/J_{\parallel} for different values of the rescaling parameter γ . Also shown is the perturbation theory result.

which are plotted in figure 2. The larger the ratio of J_{\perp}/J_{\parallel} , the closer the two critical points are. This means that the critical points H_{c1} and H_{c2} cannot be distinguished for a very large energy gap. Once the gap is closed by an external field, the ground state immediately becomes fully polarized. This is evident in the strong coupling compound $(5\text{IAP})_2\text{CuBr}_4 \cdot 2\text{H}_2\text{O}$ [5]. Here the gap opens only if $J_{\perp}/J_{\parallel} \geq 4/\gamma$, with γ arbitrary. Therefore the gap opens for arbitrary J_{\perp}/J_{\parallel} .

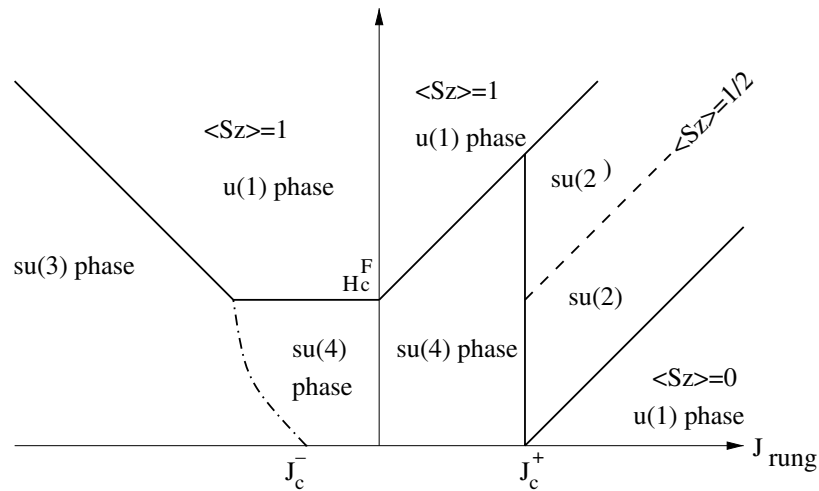


Figure 3. The magnetic phase diagram of the two-leg $su(4)$ ladder. In the antiferromagnetic regime the thick lines are $h = J_{\perp} - 4J_{\parallel}/\gamma$, $h = J_{\perp} + 4J_{\parallel}/\gamma$ and the broken line is $h = J_{\perp}$. In the ferromagnetic regime the thick lines are $h = -J_{\perp}$ and $h = 4J_{\parallel}/\gamma$. The chain line is an approximate boundary between the $su(4)$ and $su(3)$ phases.

Finally, we show the phase diagram in the presence of a magnetic field in figure 3. In the ferromagnetic rung coupling regime, the fully polarized ferromagnetic state lies in the region $h \geq |J_{\perp}|$ and $h \geq 4J_{\parallel}/\gamma$, whereas the $su(3)$ Luttinger magnetic phase is in the region $h < |J_{\perp}|$ and left of the boundary between the $su(3)$ and $su(4)$ phases. The $su(4)$ phase is in the region $h < 4J_{\parallel}/\gamma$ and right of this boundary. In the antiferromagnetic rung coupling regime, the singlet rung state lies in the region $h < J_{\perp} - 4J_{\parallel}/\gamma$ whereas the ferromagnetic fully polarized state is in the region $h \geq J_{\perp} + 4J_{\parallel}/\gamma$. The $su(2)$ magnetic phase remains in the region $h > J_{\perp} - 4J_{\parallel}/\gamma$, $h < J_{\perp} + 4J_{\parallel}/\gamma$ and $J_{\perp} \geq 4J_{\parallel}/\gamma$. The $su(4)$ magnetic phase lies in the region $h < J_{\perp} + 4J_{\parallel}/\gamma$ and $0 < J_{\perp} < 4J_{\parallel}/\gamma$.

To conclude, we have studied the phase diagram of the integrable $su(4)$ spin ladder model (1) by means of the TBA. In particular, the critical behaviour at the critical points H_{c1} and H_{c2} was derived. In the presence of a strong magnetic field, the phase diagram is in good agreement with the experimental observations for the strong coupling compounds $(5IAP)_2CuBr_4 \cdot 2H_2O$ [5], $Cu_2(C_5H_{12}N_2)_2Cl_4$ [3] and $(C_5H_{12}N)_2CuBr_4$ [4]. We have also predicted the spin gap $\Delta \approx J_{\perp} - \frac{1}{2}J_{\parallel}$ for the weak coupling compounds with $J_{\perp} \sim J_{\parallel}$, such as $(VO)_2P_2O_7$ and also shown that the gap opens for arbitrary J_{\perp}/J_{\parallel} .

Acknowledgments

The authors thank the Australian Research Council for support. AF and XWG thank I Roditi and Z-J Ying for helpful discussions as well as FAPERGS for financial support.

References

- [1] Dagotto E and Rice T M 1996 *Science* **271** 618
Dagotto E 1999 *Rep. Prog. Phys.* **62** 1525
- [2] Azuma M, Hiroi Z, Takano M, Ishida K and Kitaoka Y 1994 *Phys. Rev. Lett.* **73** 3463

- [3] Chaboussant G *et al* 1997 *Phys. Rev. Lett.* **79** 925
Chaboussant G *et al* 1998 *Phys. Rev. Lett.* **80** 2713
Chaboussant G *et al* 1997 *Phys. Rev. B* **55** 3046
- [4] Watson B C *et al* 2001 *Phys. Rev. Lett.* **86** 5168
- [5] Landee C P, Turnbull M M, Galeriu C, Giantsidis J and Woodard F M 2001 *Phys. Rev. B* **63** 100402
- [6] Tanaka H, Takatsu K, Shiramura W and Ono T 1996 *J. Phys. Soc. Japan* **65** 1945
Nakamura T and Okamoto K 1998 *Phys. Rev. B* **58** 2411
- [7] Shiramura W *et al* 1997 *J. Phys. Soc. Japan* **66** 1900
- [8] Nersesyan A A and Tselik A M 1997 *Phys. Rev. Lett.* **78** 3939
Kolezhuk A K and Mikeska H-J 1998 *Phys. Rev. Lett.* **80** 2709
- [9] Zheng W, Singh R R P and Oitmaa J 1997 *Phys. Rev. B* **55** 8052
- [10] Dagotto E, Riera J and Scalapino D 1992 *Phys. Rev. B* **45** 5744
- [11] Reigrotzki M, Tsunetsugu H and Rice T M 1994 *J. Phys.: Condens. Matter* **6** 9235
Giamarchi T and Tselik A M 1999 *Phys. Rev. B* **59** 11398
- [12] Totsuka K 1998 *Phys. Rev. B* **57** 3454
Barnes T and Riera J 1994 *Phys. Rev. B* **50** 6817
- [13] Wang Y 1999 *Phys. Rev. B* **60** 9236
- [14] Batchelor M T and Maslen M 1999 *J. Phys. A: Math. Gen.* **32** L377
Frahm H and Kundu A 1999 *J. Phys.: Condens. Matter* **11** L557
de Gier J, Batchelor M T and Maslen M 2000 *Phys. Rev. B* **61** 15196
Batchelor M T, de Gier J and Maslen M 2001 *J. Stat. Phys.* **102** 559
Maslen M, Batchelor M T and de Gier J 2003 *Phys. Rev. B* **68** 024418
- [15] Zvyagin A A 1995 *Phys. Rev. B* **51** 12579
Park S and Lee K 1998 *J. Phys. A: Math. Gen.* **31** 6569
Muramoto N and Takahashi M 1999 *J. Phys. Soc. Japan* **68** 2098
Arnaudon D, Poghossian R, Sedrakyan A and Sorba P 2000 *Nucl. Phys. B* **588** 638
Sedrakyan T 2001 *Nucl. Phys. B* **608** 557
Arnaudon D, Sedrakyan A and Sedrakyan T 2002 *Preprint hep-th/0210087*
- [16] Johnston D C, Johnson J W, Goshorn D P and Jacobson A J 1987 *Phys. Rev. B* **35** 219
- [17] Hayward C A and Poilblanc D 1996 *Phys. Rev. B* **54** R12649
- [18] Sutherland B 1975 *Phys. Rev. B* **12** 3795
Schlottmann P 1992 *Phys. Rev. B* **45** 5293
- [19] Takahashi M 1971 *Prog. Theor. Phys.* **46** 401
Schlottmann P 1986 *Phys. Rev. B* **33** 4880
- [20] Lee K 1994 *J. Korean Phys. Soc.* **27** 205
- [21] de Gier J and Batchelor M T 2000 *Phys. Rev. B* **62** R3584
Cai S, Dai J and Wang Y 2002 *Phys. Rev. B* **66** 134403
- [22] Troyer M, Tsunetsugu H and Würtz D 1994 *Phys. Rev. B* **50** 13515
- [23] Chaboussant G *et al* 1998 *Eur. Phys. J. B* **6** 167